

P. Manisankar · A. Gomathi · D. Velayutham

## Oxygen reduction at the surface of glassy carbon electrodes modified with anthraquinone derivatives and dyes

Received: 19 July 2004 / Revised: 5 August 2004 / Accepted: 10 October 2004 / Published online: 12 May 2005  
© Springer-Verlag 2005

**Abstract** The preparation, electrochemical and catalytic behaviour of glassy carbon electrodes modified by anthra-9,10-quinone, its amino derivatives and dyes were investigated. The stability of the modified electrodes was studied by cyclic voltammetry in acidic and neutral media. The electrocatalytic ability of the modified electrodes for the reduction of dioxygen to hydrogen peroxide was examined by cyclic voltammetry, chronoamperometry and chronocoulometry techniques. The influence of pH on the electrochemical and catalytic behaviour was studied and pH 5.0–8.0 was chosen as the optimum working pH by comparing the shift in oxygen reduction potential. The anthraquinone-adsorbed glassy carbon electrodes possess excellent electrocatalytic abilities for dioxygen reduction with overpotential ranging from 280 to 560 mV lower than that at a plain glassy carbon electrode. Hydrodynamic voltammetric studies were performed to determine the heterogeneous rate constants for the reduction of O<sub>2</sub> at the surface of the modified electrodes, mass specific activity of the anthraquinones used and the apparent diffusion coefficient of O<sub>2</sub> in buffered aqueous O<sub>2</sub>-saturated solutions. Studies showed the involvement of two electrons in dioxygen reduction.

**Keywords** Dioxygen reduction · Electrocatalytic reduction · Glassy carbon · Anthraquinone

### Introduction

Dioxygen reduction has been a subject of considerable interest over the past two decades, due to its involvement

in energy conversion and storage [1–3]. The current research involves the utilization of modified electrodes [4–6] which have been constructed by immobilizing the electrocatalysts at the electrode surface and facilitating the electron transfer rate in slow electrochemical reactions. In this connection, a wide variety of compounds such as manganese oxide [7], pyrimidine bases [8], copper [9], ruthenium–iron cluster [10] metal phthalocyanine [11], metal macrocyclic complexes [12], titanium silicates [13], Au nanoparticle [14], naphthoquinone [15, 16] and anthraquinone [17–20] derivatives have been proposed as electrocatalysts for the reduction of dioxygen to water or H<sub>2</sub>O<sub>2</sub>.

Anthra-9,10-quinones (AQNEs) are interesting compounds for investigations in electroanalytical chemistry due to the formation of conductive, electroactive films and monolayers [21], which make them as a key constituent, used for the modification of electrodes [22]. They have strong adsorption tendencies on various electrode materials viz. Pt [23], Hg [24], graphite [25, 26] and glassy carbon [27]. It has been shown that the preanodized glassy carbon electrode enhances the quinone–hydroquinone adsorption on the electrode's surface [28]. The adsorbed 1,4-dihydroxy anthra-9,10-quinone derivatives [19] and anthraquinone podands [20] on glassy carbon electrodes showed excellent electrocatalytic ability for the reduction of dioxygen to H<sub>2</sub>O<sub>2</sub> with overpotentials from 560 to 650 mV at pH 6.0–7.0 and from 380 to 470 mV at pH 4.5, respectively, lower than that of a plain glassy carbon electrode.

In this direction, we employed AQNE, its amino derivatives and dyes (Fig. 1) for the modification of glassy carbon electrodes. When adsorbed on the surface of preanodized glassy carbon electrodes, the used anthraquinones revealed enhanced catalytic activity for the dioxygen reduction. In this article, we discuss the electrochemical behaviour, efficiency and stability of the resulting modified electrodes in the electrocatalysis of dioxygen reduction by cyclic voltammetry, chronoamperometry, chronocoulometry and rotating-disk

P. Manisankar (✉) · A. Gomathi  
Department of Industrial Chemistry, Alagappa University,  
Karaikudi, 630003, Tamil Nadu, India  
E-mail: pms11@rediffmail.com  
Fax: +91-4565-225202

D. Velayutham  
Central Electrochemical Research Institute, Karaikudi, 630006,  
Tamil Nadu, India

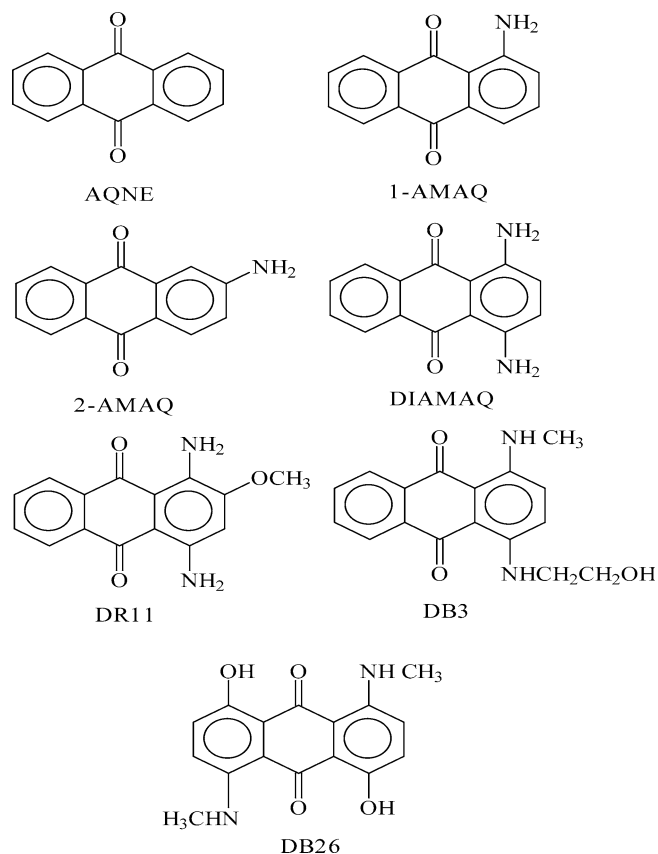


**Fig. 1** Structures of the anthraquinone derivatives and dyes used

electrode voltammetry techniques along with the determination of diffusional and kinetic parameters, characteristic of the electrode process.

## Experimental

### Chemicals

AQNE, 1-amino anthra-9,10-quinone (1-AMAQ), 2-amino anthra-9,10-quinone (2-AMAQ) and 1,4-diamino anthra-9,10-quinone (DIAMAQ) were purchased from Lancaster. 1-[(2-hydroxy ethyl) amino]-4-(methyl amino) anthra-9,10-quinone (DB3), 1,5-dihydroxy-4,8-bis(methyl amino)anthra-9,10-quinone (DB26) and 1,4-diamino-2-methoxy anthra-9,10-quinone (DR11) were received as samples from ATUL India Ltd. and purified before use. HPLC grade acetonitrile (SRL) was used as received. Triply distilled water was deionized using TKA water purifier and used throughout the experiments. All chemicals used were of the highest purity available from Merck. The aqueous solutions used at different pH values were 0.1 M  $\text{H}_2\text{SO}_4$  (pH 1.0), 0.1 M  $\text{H}_2\text{SO}_4$  + 0.1 M NaOH (pH 2.0–3.0), 0.2 M  $\text{CH}_3\text{COOH}$  + 0.2 M  $\text{CH}_3\text{COONa}$  (pH 3.5–5.5), 0.1 M  $\text{NaH}_2\text{PO}_4$  + 0.1 M NaOH (pH 6.0–12.0) and 0.1 M NaOH (pH 13.0). The above pH solutions were prepared by adding suitable

quantities of acid or alkali and checking the pH of the medium using Cyberscan 500-pH meter.  $\text{N}_2$  and  $\text{O}_2$  gases with purity 99.999% were used during the experiments. The deposition solutions of  $4.53 \times 10^{-3}$  mol  $\text{dm}^{-3}$  of AQNE,  $9.02 \times 10^{-3}$  mol  $\text{dm}^{-3}$  of 1-AMAQ,  $4.99 \times 10^{-3}$  mol  $\text{dm}^{-3}$  of 2-AMAQ,  $5.14 \times 10^{-3}$  mol  $\text{dm}^{-3}$  of DIAMAQ,  $5.05 \times 10^{-3}$  mol  $\text{dm}^{-3}$  of DR11,  $5.15 \times 10^{-3}$  mol  $\text{dm}^{-3}$  of DB3 and  $5.12 \times 10^{-3}$  mol  $\text{dm}^{-3}$  of DB26 were prepared, based on their solubility in acetonitrile.

### Electrode preparation

The glassy carbon electrode (GCE, EG&G, 0.0314  $\text{cm}^2$  area) was polished mechanically with alumina powder (0.5  $\mu\text{m}$ ) for 5 min and then ultrasonicated to remove any powder material adhered to the electrode surface. Finally, the electrode was thoroughly degreased with trichloroethylene and washed with deionized water and acetone. Preanodization of glassy carbon electrodes was carried out by continuous potential cycling between 1.8 and  $-0.5$  V at a sweep rate of 100  $\text{mV s}^{-1}$  in 0.5 mol  $\text{dm}^{-3}$   $\text{H}_2\text{SO}_4$  solution until a stable voltammogram was obtained. The preanodized glassy carbon electrode was then placed in the deposition solutions at open circuits for varying time periods (2–4 h) [29]. The resulting modified electrode was rinsed thoroughly with deionized water.

A three-electrode cell with a saturated calomel reference electrode (SCE), a platinum wire counter electrode and a modified glassy carbon working electrode was employed.

### Procedure

Cyclic voltammetric experiments were carried out on a modified glassy carbon electrode in 15 ml aqueous pH solution which was deaerated by purging  $\text{N}_2$  gas for 10 min. Consequently, the same experiments were repeated after purging  $\text{O}_2$  gas for 10 min. Hydrodynamic voltammetric experiments were done on the modified GCE in 100 ml aqueous pH solution deaerated by purging  $\text{N}_2$  gas for 40 min and in the presence of oxygen by purging  $\text{O}_2$  gas for 20 min. Deaeration by  $\text{N}_2$  gas lesser than 40 min led to characteristic response in the voltammogram. All electrochemical experiments were carried out at a thermostatic temperature of  $25.0 \pm 0.1$  °C.

### Apparatus

Cyclic voltammetry, chronoamperometry and chronocoulometry were performed on an EG&G Princeton Applied Research Model 273A potentiostat/galvanostat (Princeton, NJ, USA) controlled by M270 software. A bi-potentiostat model AFRDE5 having an analytical rotator model AFMSRXE with MSRX speed control

(PINE Instruments, USA) was employed for hydrodynamic voltammetric studies on dioxygen reduction.

## Results and discussion

Glassy carbon electrodes were modified with AQNE, its amino derivatives and dyes by keeping the preanodized electrodes at open circuits in anthraquinone solutions in acetonitrile. All voltammetric studies of the resulting modified glassy carbon electrodes were performed under deaerated and oxygen saturated conditions at various pH media in the range 1.0–13.0.

Voltammetric behaviour of the GC electrodes modified with AQNEs

Cyclic voltammograms of GCE modified with AQNE, 1-AMAQ, 2-AMAQ, DIAMAQ and DB3 exhibited a single redox couple in the deaerated solution whereas GCE modified with DR11 and DB26 showed an irreversible cathodic peak at pH 1.0. These voltammograms at various scan rates were studied to examine the variation of peak current with scan rate. Figure 2 shows the cyclic voltammetric response of GCE modified by 1-AMAQ in a  $0.1 \text{ mol dm}^{-3} \text{ H}_2\text{SO}_4$  solution at various scan rates and the inset exhibits the plot between cathodic peak current and scan rate. The cathodic peak current  $I_{pc}$  varies linearly with scan rate  $v$ , as predicted for a diffusionless system. Non-linear variation of  $I_{pc}$  with  $v^{1/2}$  and slope values around 0.7 for a straight line obtained in the correlation between  $\log I_{pc}$  and  $\log v$  ( $y = 0.6689x - 0.9619$ ;  $R^2 = 0.9844$ ) confirm the diffusionless process. But small diffusional tails appear for all the amino anthraquinone derivatives and dyes except for AQNE which may be due to the diffusion of few protonated amino anthraquinone molecules under acidic conditions. An increase in peak separation with increase in scan rate proves the quasi-reversibility of the electron transfer process. Similar electrochemical behaviour was

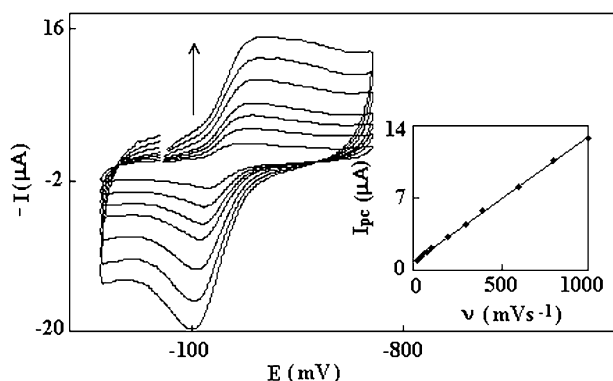


**Fig. 2** Cyclic voltammograms for 1-AMAQ adsorbed on a glassy carbon electrode in  $0.1 \text{ mol dm}^{-3} \text{ H}_2\text{SO}_4$  aqueous solution at scan rates 100, 200, 300, 400, 600, 800 and  $1,000 \text{ mV s}^{-1}$ . The inset shows the plot of the cathodic peak current vs scan rates

observed for the case of other anthraquinone derivatives and dyes.

### Effect of pH

Our results exhibited the pH dependence of the voltammetric peak potentials, i.e., the anodic and cathodic peak potentials shift toward more negative values by increasing pH of the solution. The half-peak potential  $E_{p/2}$  vs pH plot consisted two distinct linear portions with different slopes of 62 mV at pH values 1.0–9.0 (two-electron, two-proton process leads to hydroquinone) and 30 mV at pH values above 9.0 (two-electron, one-proton process leads to hydroquinone anion) per unit change in pH for AQNE. Three distinct linear segments with different slopes of 88–92 mV at low pH values (two-electron, three-proton process leads to protonated hydroquinones), 56–62 mV at intermediate pH values (two-electron, two-proton process leads to hydroquinones) and 28–32 mV at high pH values above 9.0 (two-electron, one-proton process leads to hydroquinone anion) per unit change in pH were observed for the remaining six amino anthraquinone derivatives and dyes. At low pH values, the protonation of the second amino group in DIAMAQ, DB3, DB26 and DR11 may be difficult due to the electron withdrawing quaternary ammonium cation present in protonated anthraquinones. A sample half-peak potential vs pH plot for DIAMAQ is shown in Fig. 3. Moreover, it is interesting to note that there is a gradual decrease in the surface coverage of the modified electrodes by increasing the pH of the solution. Cyclic voltammograms obtained at  $\text{pH} > 9.0$  showed a dramatic loss in the electrode's surface coverage and poorly defined waves. This is most probably due to either displacement of the adsorbed material by anions that are part of the buffer systems or, alternatively due to hydrolysis of the adsorbed anthraquinones at high pH values [19, 20].

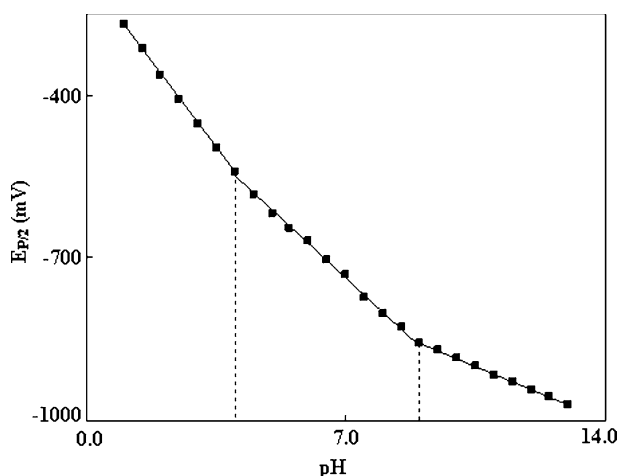


**Fig. 3** pH-potential diagram for DIAMAQ adsorbed on a glassy carbon electrode

### Effect of substituents

In order to examine the influence of AQNE substituents on the electrochemical properties, the  $E_{P/2}$  values were evaluated at a pH of 7.0 at which all anthraquinones used are reduced in a two-electron, two-proton process. The resulting  $E_{P/2}$  values are summarized in Table 1. The reduction potential of anthraquinones is in the order AQNE < 2-AMAQ < 1-AMAQ < DB26 < DIAMAQ < DB3 < DR11. As is obvious from the data, reduction potential is shifted negatively by electron donating substituents. The unsubstituted anthraquinone reduces at lower potential than the amino substituted derivatives and dyes. 1-AMAQ reduces at a more negative potential (36.3 mV) compared with 2-AMAQ. This is most probably due to the possible intramolecular H-bonding between the  $-\text{NH}_2$  and  $-\text{CO}$  groups of 1-AMAQ which may stabilize the anthraquininoid form and is also reported in earlier literature [30]. Since DIAMAQ has two  $-\text{NH}_2$  groups adjacent to keto groups, it reduces at a still higher cathodic potential than 1-AMAQ. Although DB26 has electron donating substituents at four centres, due to steric effect, it reduces at comparatively lesser potential than DIAMAQ, DB3 and DR11. Due to the presence of methyl substituted amino groups, DB3 reduces at higher potential in comparison with DIAMAQ. On the other hand, the presence of methoxy group, which exerts strong electron donating resonance effect, in addition to two amino groups in DR11, results in a relatively large shift towards more negative reduction potential.

### Stability of the modified electrodes

The stability of the modified electrodes and reproducibility of their electrochemical behaviour were investigated by immersing them in acidic medium (pH 1.0) for 48 h and in neutral medium (pH 7.0) for 36 h and then recording the cyclic voltammograms. A slight decrease in the corresponding voltammograms (<4%) was observed. In addition, 30 min of repetitive scanning between 0 and  $-1000$  mV at pH 7.0 including more than 40 complete cycles, revealed no measurable decrease in the peak height or separation of peaks. The reproduc-

ibility of the electrocatalytic effect of the modified electrodes was ascertained from the unaltered peak potentials and current observed in the cyclic voltammograms of 40 min of repetitive cycling at a scan rate of  $40 \text{ mV s}^{-1}$  under oxygen saturated condition at pH 7.0. After such repetitive scanning, the cyclic voltammogram was recorded under deaerated conditions and compared with the cyclic voltammogram obtained initially under deaerated conditions. A 5% decrease in the peak height with no change in the peak separation was observed. Thus the stability of the modified electrodes after the electrocatalytic studies was confirmed.

### Catalytic reduction of dioxygen at the surface of modified electrodes

#### Effect of pH

The electrocatalytic reduction of dioxygen at GCE modified with anthraquinones was also examined in various buffers between pH 1.0 and 13.0. Although the reduction potentials of both dioxygen and anthraquinones are pH-dependent [19, 20], their displacement may be unequal because of their different kinetic behaviour. Consequently, buffered solutions of pH > 3 are favourable to study the catalytic reduction of dioxygen. Thus, a pH of about 5.0–8.0 (depending on the nature of the modifying anthraquinone) was found to be the optimum pH (Table 1), where the electrode's anodic wave completely disappeared and the cathodic wave reached its maximum value and the maximum shift in oxygen reduction potential was observed. As the pH increases, the oxygen reduction potential at plain GCE increases upto pH 7.0. The oxygen reduction potential shift observed by employing anthraquinones as catalysts is the difference between the oxygen reduction potentials in the presence and absence of anthraquinones. The average values of oxygen reduction potential shifts obtained from five identical experiments (RSD 2.4%) were correlated with pH. As an example, Fig. 4 exhibits the variation of shift in dioxygen reduction potential with pH for GCE modified by DB26. Here, the maximum shift is observed at pH 7.0. For instance, cyclic voltammograms of the GCE modified by AQNE (Fig. 5) at pH 7.0 in the absence and presence of dioxygen were compared with the corresponding voltammograms at the surface of bare GCE. The dioxygen reduction at a bare GCE occurs irreversibly with a peak potential of about  $-1020.9$  mV at pH 7.0. Figure. 5b shows that there is a large enhancement in the cathodic peak current of the GCE modified with AQNE in the presence of  $\text{O}_2$ , while the corresponding anodic peak has disappeared clearly indicating the electrocatalytic reduction of dioxygen which occurs only at a peak potential of  $-577.9$  mV. Thus the GCE modified with AQNE causes the shift in oxygen reduction potential ( $\Delta E$ ) by about 443 mV. The observed shifts with the different anthraquinones investigated at their optimum pH are given in

**Table 1** Half-peak potential at pH 7.0 ( $E_{P/2}$ ), optimum pH for dioxygen reduction (pH) and dioxygen reduction potential shift ( $\Delta E$ )

Anthraquinones	$E_{P/2}$ vs SCE (mV)	pH	$\Delta E$ (mV)
AQNE	-551	7.0	443.0
1-AMAQ	-640	8.0	330.5
2-AMAQ	-604	5.0	400.1
DIAMAQ	-731	7.0	477.0
DR11	-800	5.0	280.0
DB3	-772	7.0	540.0
DB26	-696	7.0	560.1

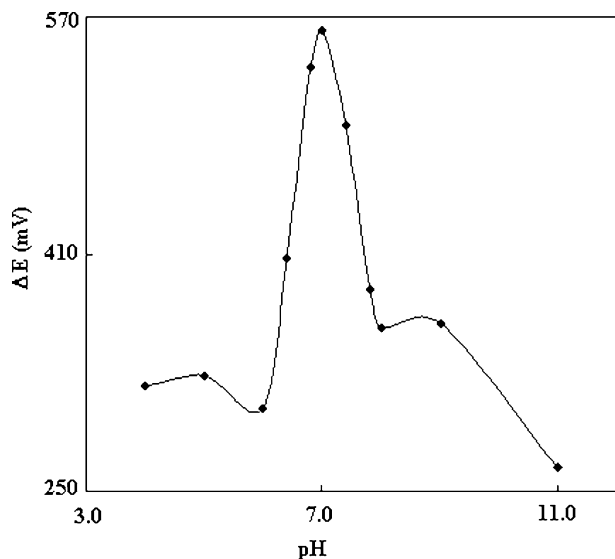


Fig. 4 Plot of pH vs.  $O_2$  reduction potential shift for the modified GCE by DB26

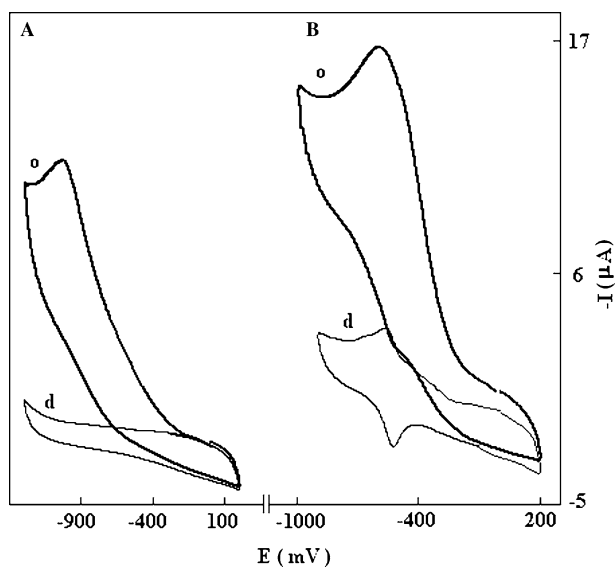


Fig. 5 (a). Cyclic voltammograms for a bare GCE at pH 7.0 (phosphate buffer) in the absence (*d*) and presence (*o*) of dioxygen, b. Same as a for a GCE modified with AQNE. Scan rate  $40 \text{ mV s}^{-1}$

Table 1. Salimi et. al. [19] also studied this reduction using GCE modified by 1,4-dihydroxy-anthra-9,10-quinone derivatives at pH 6.0–7.0. It was reported recently [31] that dioxygen is reduced bioelectrocatalytically to water at neutral pH.

#### Effect of scan rate

The variation of cathodic peak current with scan rate was also investigated for GCE modified with different anthraquinones under  $O_2$  saturated conditions. Here the cathodic peak current  $I_{pc}$  is directly proportional to

square root of the scan rate  $v^{1/2}$  which indicates that at sufficient overpotentials the reaction is transport limited [1, 20]. The results obtained so far show that the overall electrochemical reduction of dioxygen at the modified electrodes introduced might be controlled by the diffusion of  $O_2$  in solution and by the cross-exchange process between  $O_2$  and the redox sites of the anthraquinone derivatives and dyes used.

#### Effect of substituents

In order to investigate the influence of AQNE substituents in the electrocatalytic properties, the maximum shifts in dioxygen reduction potential by GCE modified with anthraquinones, which have the identical optimum pH, were compared. The shift is in the order DB26 > DB3 > DIAMAQ > AQNE. In the mechanism already reported [19, 20] the presence of electron donating substituents exerting mesomeric effect decreases the stability of hydroquinone obtained in the first step, thereby facilitating the reduction of dioxygen in the second step by releasing hydrogens easily from hydroquinone to form hydrogen peroxide. Hence the AQNE causes a lesser shift in dioxygen reduction potential than DIAMAQ. Due to the alkyl substitution in amino groups, which facilitates the mesomeric effect exerted by amino group, DB3 causes greater shift than DIAMAQ. Two hydroxyl groups being electron-rich, which exert mesomeric effect in addition to two methylated amino groups, bring the higher shift in DB26 than DB3.

#### Chronoamperometry

The chronoamperometric behaviour of bare and modified GCEs by anthraquinones used was investigated in the absence and presence of  $O_2$ . The double potential-step technique at an initial and final potential of  $-300$  and  $-750 \text{ mV vs SCE}$  was employed for this purpose. For instance, chronoamperograms of bare GCE and modified GCE by AQNE in the presence and absence of  $O_2$  are illustrated in Fig. 6a and b, respectively. The net electrolysis current  $I_{net}$  was determined by point-to-point subtraction of the background current in the presence and absence of  $O_2$ . In deoxygenated buffer, a plot of net current against  $t^{-1/2}$  shows a straight line (Fig. 6c line *d*) which extrapolates close to the origin. Since the oxidized and reduced forms of the anthraquinone derivatives are known to be insoluble in water, such a near-Cottrellian behaviour may be explained by finite diffusion in thin films [1, 15, 16, 20]. But on oxygen saturation, the corresponding Cottrell plot,  $I_{net}$  vs  $t^{-1/2}$  (Fig. 6c line *o*) is linear at short time periods, while it deviates from linearity at longer times. The extrapolation of the linear part of the plot  $I_{net}$  vs  $t^{-1/2}$  will result in an intercept at about  $-12.09 \mu\text{A}$ . This transient current seems to be largely due to the catalytic reduction of dioxygen by the anthraquinone used. A similar behaviour

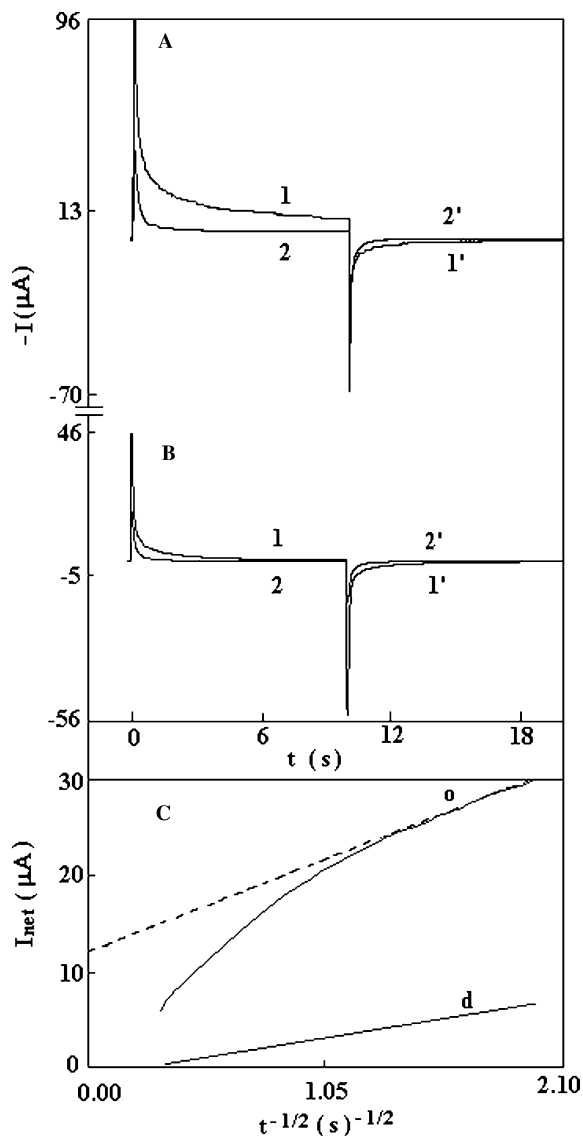


**Fig. 6** Chronoamperograms obtained in pH 7.0 by the double potential-step technique at an initial potential of  $-300$  mV and final potential of  $-750$  mV vs SCE (a). 1,1' for a GCE modified with AQNE in the  $O_2$ -saturated buffer. 2,2' as 1,1' for the bare GCE. b. 1,1' for a GCE modified with AQNE in the absence of dioxygen, 2,2' as 1,1' for the bare GCE. c. Plots of net current vs  $t^{-1/2}$  for the GCE modified with AQNE in the absence (d) and presence (o) of dioxygen

was also observed for other anthraquinone derivatives and dyes.

### Chronocoulometry

Double potential-step chronocoulometric studies were carried out at bare GCE and anthraquinone-modified GCE in the absence and presence of oxygen. The initial and final potentials are the same as in the chronoamperometric studies. An example of chronocoulomogram for GCE modified by 2-AMAAQ is presented in Fig. 7. In oxygenated buffer, there is a large enhancement in

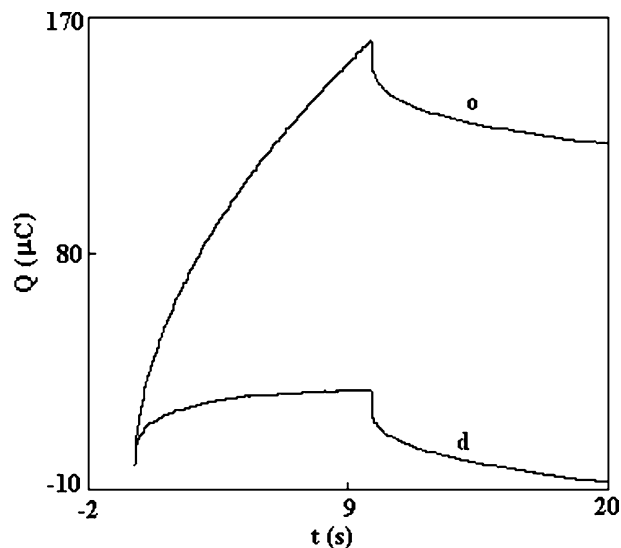


**Fig. 7** Chronocoulometric curves of GCE modified with 2-AMAAQ by the double potential-step technique at an initial potential of  $-300$  mV and final potential of  $-750$  mV vs SCE at pH 5.0 in the absence (d) and presence (o) of dioxygen

charge and when the potential is reversed, a nearly flat line appears indicating the irreversible electrocatalytic reduction of dioxygen. The same trend was observed for the other anthraquinone derivatives and dyes.

### Hydrodynamic voltammetric studies on dioxygen reduction

The analysis of the electrocatalytic process of dioxygen reduction at the modified electrodes by cyclic voltammetry alone is found to be difficult because of the complexity of the rate-controlled process. However, using rotating disk electrodes and keeping the electrodes at a stationary potential a steady state can be attained. Thus the rates of mass transfer at the surface of a rotating disk electrode would be much greater than those of charge transfer. Subsequently, the relative contribution of the effect of mass transfer to the electron transfer kinetics will be smaller.

Thus the electrocatalytic reduction of  $O_2$  was examined with the GC rotating electrodes modified by anthraquinone derivatives and dyes used at their optimum pH to obtain the kinetic parameters. As an example, Fig. 8a shows a set of current-potential curves recorded in an  $O_2$ -saturated buffer of pH 8.0 at various angular velocities  $\omega$ , with a rotating disk GCE on which  $1.01 \times 10^{-9}$  mol  $cm^{-2}$  of 1-AMAAQ was adsorbed. Curve (a) shows the residual current due to the reduction of anthraquinone at modified electrode in the absence of  $O_2$ . The limiting current  $I_l$  is defined as the difference between the currents on a modified electrode at the potential corresponding to the diffusion plateau in de-aerated and  $O_2$ -saturated solutions [1, 15, 16, 20]. The mass specific activity or current of anthraquinone which

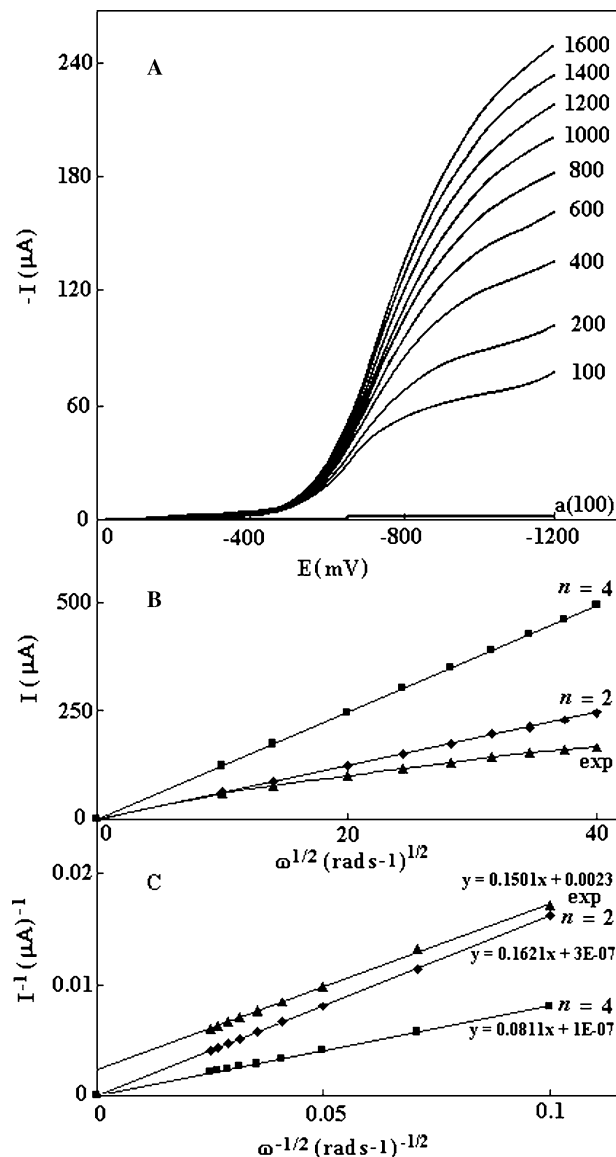


**Fig. 8** a Current–potential curves for the reduction of  $O_2$  (1.25 mM) at a rotating glassy carbon electrode modified with 1-AMAQ in the buffered solution of pH 8.0 at different rotation rates (rpm) and scan rate of  $20 \text{ mV s}^{-1}$ . b. Levich plot of limiting currents at  $-950 \text{ mV}$  (exp), and theoretical Levich plots for two ( $n=2$ ) and four ( $n=4$ ) electron reduction of  $O_2$  and c. Koutecky–Levich plots of the above data

is defined as current response of the catalyst per mg in dioxygen reduction at  $\omega=100 \text{ rpm}$  was determined [32] and is represented in Table 2. The Levich and Koutecky–Levich plots were derived from the current–potential curves at various angular velocities and are shown in Fig. 8b and c, respectively. The Levich plot, derived from the limiting current measured at a potential of  $-950 \text{ mV}$  (Fig. 8b), is very close to the theoretically calculated line for a two-electron process ( $n=2$ ) and shows a slight negative deviation at higher  $\omega$  values. Such non-linearity may be the result of catalytic reduction in which a current-limiting chemical step precedes

the electron transfer. Earlier reports also showed similar results in the literature [1, 15, 19, 20]. However, the corresponding Koutecky–Levich plot (Fig. 8c) is linear, with a slope close to that of the theoretical line for the reduction of  $O_2$  via two electrons, indicating that the adsorbed catalyst accomplished the reduction of  $O_2$  to  $H_2O_2$ . Similar behaviour was observed in the case of other AQNE derivatives and dyes.

The rate constant for the catalytic reaction between the reduced anthraquinone AQH<sub>2</sub> and  $O_2$  ( $AQH_2 + O_2 \rightarrow H_2O_2 + AQ$ ) is obtained from the Koutecky–Levich plots using the following expression:

$$I_1^{-1} = I_k^{-1} + I_{\text{lev}}^{-1} \\ = [nFAkC_{O_2}\Gamma_{\text{Aq}}]^{-1} + \left[0.62nFAD_{O_2}^{2/3}v^{-1/6}\omega^{1/2}C_{O_2}\right]^{-1}$$

where  $C_{O_2}$  is the bulk concentration of  $O_2$ ,  $\omega$  is the rotational speed,  $v$  is the hydrodynamic viscosity,  $\Gamma_{\text{Aq}}$  is the electrode surface coverage of the corresponding anthraquinone,  $k$  is the rate constant and all the remaining parameters have their usual meanings. The surface coverage  $\Gamma$  can be evaluated from the equation  $\Gamma = Q/nFA$  where  $Q$  is the charge obtained by integrating the cathodic peak after the background correction at low scan rate of  $10 \text{ mV s}^{-1}$  and the other symbols have their usual meanings. The calculated  $\Gamma$  values for all anthraquinones are included in Table 2. The rate constants for the dioxygen reduction were evaluated from the intercepts of the Koutecky–Levich plots and are reported in Table 2. The diffusion coefficient of  $O_2$  at rotating GCE modified with anthraquinones in oxygen-saturated aqueous buffer was determined using the Levich equation and are summarized in Table 2. The values of kinematic viscosity of water  $\nu$ , and the concentration of  $O_2$  in solution  $C_{O_2}$  used in this calculation were  $0.01 \text{ cm}^2 \text{ s}^{-1}$  and  $1.25 \text{ mM}$  [1, 19, 20], respectively.

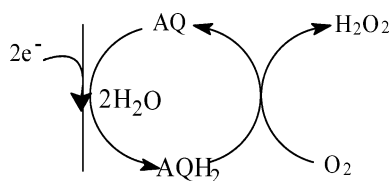
## Conclusions

AQNE, its amino derivatives and dyes were used to modify GCEs for the electrocatalytic reduction of  $O_2$ . The electrocatalytic properties of modified electrodes

**Table 2** Surface coverage ( $\Gamma$ ), mass specific activity or current (MSC), Heterogeneous rate constant ( $k$ ) and diffusion coefficient ( $DO_2$ ) of  $O_2$  in the electrocatalytic reduction of  $O_2$  at the surface of GC electrodes modified by anthraquinones used

Anthraquinones	$10^9 \Gamma$ (mol cm <sup>-2</sup> )	MSC (A mg <sup>-1</sup> )	$10^{-4} k$ (M <sup>-1</sup> s <sup>-1</sup> )	$10^5 DO_2$ (cm <sup>2</sup> s <sup>-1</sup> )
AQNE	0.78	10.01	6.08	1.412
1-AMAQ	1.01	8.27	5.68	1.729
2-AMAQ	2.53	3.28	2.61	1.665
DIAMAQ	1.93	3.94	3.11	1.571
DR11	2.92	2.13	1.37	1.560
DB3	2.94	1.96	1.45	1.596
DB26	2.83	2.19	2.33	1.645

were studied by cyclic voltammetry, chronocoulometry and chronoamperometry. Anthraquinones were strongly and irreversibly adsorbed on preanodized GCE surfaces. Under deaerated conditions, the reduction potential of the modified electrodes was shifted toward more negative direction with increasing pH of the media. The modified GCEs by anthraquinones exhibited potent electrocatalytic activities towards dioxygen reduction in buffer solution of pH 5.0–8.0 with an overpotential of about 280–560 mV lower than at a plain GCE. This oxygen reduction potential shift is greater than the shift observed for AQNE podands [20] and slightly lower than for 1,4-dihydroxy 9,10-anthraquinones [19]. The kinetic parameters such as mass specific activity of catalysts, electrocatalytic reaction rate constant and diffusion coefficient of dioxygen were evaluated from rotating-disk voltammetric measurements. The rate constant  $k$  values are greater than the values obtained for 1,4-dihydroxy 9,10-anthraquinones and comparable with that of anthraquinone podands. The diffusion coefficient values of oxygen obtained are also comparable with earlier reports [15, 19, 20]. Since hydrodynamic voltammetric studies showed the involvement of two electrons, the dioxygen reduction catalysed by AQNEs is depicted as follows:



## References

- Salimi A, Ghadermazi M (2001) *Anal Sci* 17:1165
- Williams MC (ed) (2000) *Fuel cell handbook*, 5th edn. US Department of Energy, Washington, pp 1–37
- Lai ME, Bergel A (2000) *J Electroanal Chem* 494:30
- Paulus UA, Schmidt TJ, Gasteiger HA, Behm RJ (2001) *J Electroanal Chem* 495:134
- Ohde H, Maeda K, Yoshida Y, Kihara S (2000) *J Electroanal Chem* 483:108
- Shi C, Anson FC (2000) *J Electroanal Chem* 484:144
- Mao L, Zhang D, Sotomura T, Nakatsu K, Koshiba N, Ohsaka T (2003) *Electrochim Acta* 48:1015
- Peressini S, Tavagnacco C, Costa G, Amatore C (2002) *J Electroanal Chem* 532:295
- Vukmirovic MB, Vasiljevic N, Dimitrov N, Sieradzki K (2003) *J Electrochem Soc* 150 (1):B10–B15
- Gonzalez-Cruz R, Solorza-Feria O (2003) *J Solid State Electrochem* 7:289
- Ramirez G, Trollund E, Isaacs M, Armijo F, Zagal J, Costamagna J, Aguirre MJ (2002) *Electroanalysis* 14:540
- Lin AS, Huang JC (2003) *J Electroanal Chem* 541:147
- Chithra R, Renuka R (2003) *J Appl Electrochem* 33:443
- Zhang Y, Asahina S, Yoshihara S, Shirakashi T (2003) *Electrochim Acta* 48:741
- Manisankar P, Mercy Pushpalatha A, Vasanthkumar S, Gomathi A, Viswanathan S (2004) *J Electroanal Chem* 571:43
- Golabi SM, Raoof JB (1996) *J Electroanal Chem* 416:75
- Sarapuu A, Vaik K, Schiffrin DJ, Tammeveski K (2003) *J Electroanal Chem* 541:23
- Tammeveski K, Kontturi K, Nichols RJ, Potter RJ, Schiffrin DJ (2001) *J Electroanal Chem* 515:101
- Salimi A, Mousavi MF, Sharghi H, Shamsipur M (1999) *Bull Chem Soc Jpn* 72:2121
- Salimi A, Eshghi H, Sharghi H, Golabi SM, Shamsipur M (1999) *Electroanalysis* 11:114
- Zon A, Palys M, Stojek Z, Sulowska H, Ossowski T (2003) *Electroanalysis* 15:579
- Hu SS, Xu CL, Wang GP, Cui DF (2001) *Talanta* 54:115
- Soriaga MP, Hubbard AT (1982) *J Am Chem Soc* 104:2735
- He P, Crooks RM, Faulkner LR (1990) *J Phys Chem* 94:1135
- Zhang J, Anson FC (1992) *J Electroanal Chem* 331:945
- McDermott MT, Kneten K, McCreery RL (1992) *J Phys Chem* 96:3124
- Mohan TM, Gomathi H, Rao GP (1990) *Bull Electrochem* 6:630
- Gomathi H, Rao GP (1985) *J Electroanal Chem* 85:190
- Shiu KK, Song F, Dai HP (1996) *Electroanalysis* 8:1160
- Shamsipur M, Salimi A, Golabi SM, Sharghi H, Mousavi MF (2001) *J Solid State Electrochem* 5:68
- Tsujimura S, Tatsumi H, Ogawa J, Shimizu S, Kano K, Ikeda T (2001) *J Electroanal Chem* 496:69
- Brankovic SR, Wang JX, Adzic RR (2001) *Electrochem Solid State Lett* 4:A217